First-order perturbation approach to elliptic winding deformations

M. Dalarsson [1] and M. Norgren [2]

Division of Electromagnetic Engineering, Royal Institute of Technology
Stockholm SE-100 44, Sweden
[1] mariana.dalarsson@ee.kth.se
[2] martin.norgren@ee.kth.se

***Abstract*—We apply a novel on-line method to detect elliptic deformations of winding turns in a power transformer. We employ the first-order perturbation theory to a transformer winding surrounded by the transformer tank wall and the magnetic core. The transformer winding is modeled as a structure consisting of thin conducting cylindrical rings (winding segments or turns) situated within a coaxial cylindrical waveguide, where the inner conducting cylinder represents the magnetic core and the outer conducting cylinder represents the wall of the transformer tank. We simulate antennas inside the transformer tank to radiate and measure microwave fields, in order to identify and quantify elliptic deformations of the individual winding segments or individual turns. The propagation problem is solved by conventional waveguide theory, including mode-matching and cascading techniques. We utilize optimization to solve the inverse problem and obtain a good agreement between the reconstructed and true deformations of the winding segments.**

I. I

Power transformers are critical components of power grids. While in operation, transformers are subject to degradation, including thermal hot spots, winding deformations by mechanical forces, and moisture in the insulation due to decomposition. Degradation effects are detected using diagnostic methods. However, the existing methods are often inaccurate or only applicable off-line. Off-line methods generally imply a non-service stress of a transformer [1], [2], [3], [4]. On the other hand, on-line monitoring methods of winding deformations due to the mechanical forces from short circuit currents are generally not available.

In this paper we study an on-line method to detect the mechanical deformations where one or more winding segments (or turns) have been slightly deformed from the ideal circular form to an elliptic form. Our general method [5] can in principle also be used to detect the effects of other types of degradation mechanisms (see e.g. [6]), but the investigation in the present paper focuses on a specific class of mechanical deformations only.

The idea of our approach is to insert antennas inside the transformer tank, above and below the transformer windings, to radiate and measure microwave fields that interact with the winding structure. The analysis of the measured signals and their relations to the structure parameters, being critical signatures of mechanical deformations, is an inverse electromagnetic problem [7] that typically is not straightforward to solve mathematically. We solve the propagation problem by conventional waveguide theory, including mode-matching and cascading techniques [8]. We use an optimization technique for solving the inverse problem in order to reconstruct the actual deformations of the irradiated winding segments.

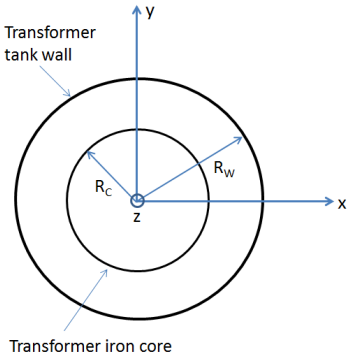

Fig. 1. The power transformer as a coaxial cylindrical waveguide.

II. T

We model a transformer winding structure as a coaxial cylindrical waveguide where the inner conducting cylinder represents the magnetic core, and the outer conducting cylinder represents the wall of the transformer tank, as shown in Fig. 1. In between there is a set of thin conducting cylindrical rings (winding segments or turns) that are situated within a coaxial cylindrical waveguide. The geometry of our model of a transformer winding surrounded by the transformer-tank wall and the magnetic core is shown in Fig. 2. We denote the four regions (1-4) between the two cylindrical conductive surfaces of the coaxial waveguide (magnetic core and tank wall) and the conductive obstacle (winding segment or turn) as indicated in Fig. 2.

For the propagation problem we only consider TM-modes ($H_z = 0$) as they include the TEM-mode, which is the dominant mode in all regions. Following [10], the longitudinal component of the electric field is given by

$$E_z = \frac{1}{\sigma + \mathrm{j}\omega\epsilon}\left(\frac{\mathrm{d}^2\Lambda}{\mathrm{d}z^2} + k^2\Lambda\right)T(r,\varphi) \quad , \tag{1}$$

where $k^2 = \mathrm{j}\omega\mu(\sigma + \mathrm{j}\omega\epsilon)$ and $\Lambda(z) = \exp(-\mathrm{j}k_z z)$ for progressive waves traveling in positive z-direction. The

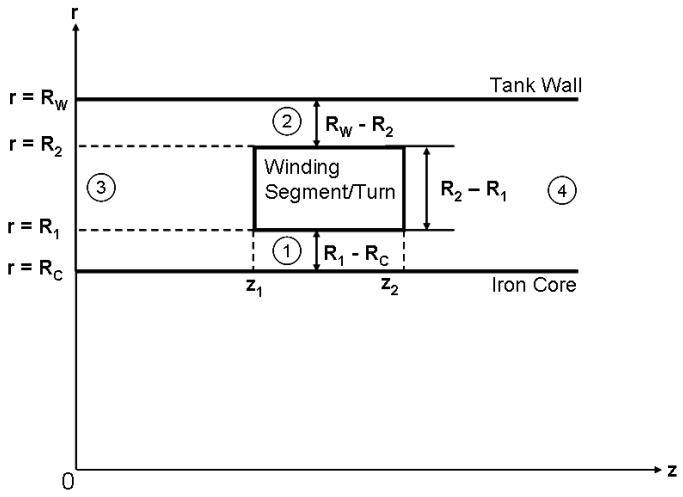

Fig. 2. Cross section of a coaxial waveguide as a model of a transformer winding.

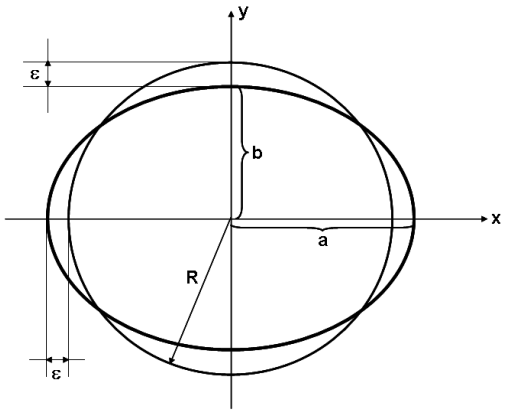

Fig. 3. Elliptic deformation of the circular winding of radius R.

material parameters μ, σ and ϵ are the effective permeability, conductivity and permittivity, respectively, for the transformer winding insulation. The scalar transverse function denoted by $T(r,\varphi)$ in (1) for TM-waves in a coaxial wave guide is a solution of the transverse wave equation

$$\nabla_T T(r,\varphi) + \gamma^2 T(r,\varphi) = 0 \quad , \tag{2}$$

where γ is the transverse wave vector. An approximate solution of the equation (2) for TM-waves, suitable for our problem, is given by [10]

$$T_{n,m}(r,\varphi) = Q \sin\frac{n\pi(r-R_I)}{R_O - R_I}\cos(m\varphi) \quad , \tag{3}$$

with

$$\gamma^2_{n,m} = \frac{n^2\pi^2}{(R_O-R_I)^2} + \frac{4m^2}{(R_I+R_O)^2} \quad , \tag{4}$$

where $n = 1, 2, \ldots$ and $m = 0, 1, 2, \ldots$ are two integers that denote the TM-modes in this case. In (3) and (4) we denote the radii of the inner and outer cylinders of the coaxial waveguide by R_I and R_O respectively.

III. T -

Let us now assume that the transformer winding segment (or turn) of radius R (equal to inner radius R_1 or outer radius R_2 according to Fig. 2 for regions 1 and 2 respectively) lying between the magnetic core of radius R_C and the transformer tank of radius R_W, is slightly deformed from the expected circular shape of radius R to an ellipse with semi-major axis a and semi-minor axis b. The ideal circular shape and the actual deformed elliptic shape of the transformer winding segment (or turn) are shown in Fig. 3.

From Fig. 3, to the first order of approximation in the small parameter ε/R, we obtain the following result for the size of the radial deformation $\delta(r,\varphi)$ of the elliptic winding compared to the unperturbed circular winding

$$\delta(r,\varphi) = \delta(\varphi) = r - R = \varepsilon\cos 2\varphi \quad . \tag{5}$$

From (5), we see that $a - R = +\varepsilon$ for the semi-major axis ($r = a$) when $\varphi = 0, \pi$ while $b - R = -\varepsilon$ for the semi-minor axis ($r = b$) when $\varphi = \pi/2, 3\pi/2$ in accordance with Fig. 3. Thus we have $a = R+\varepsilon$ and $b = R-\varepsilon$ such that, to the second order of approximation in the small parameter ε/R, the length of the perturbed ellipse is given by

$$O = 2\pi R\left(1 + \frac{\varepsilon^2}{4R^2}\right) \approx 2\pi R \quad , \tag{6}$$

and we see that up to the first order in the small parameter ε/R, the turn length of the perturbed winding is approximately equal to the turn length of the corresponding unperturbed winding. Following Jackson [9] (Problem 8.12), if the eigenvalue parameters and eigenfunctions of the transverse equation for two boundary contours C and C_0 are (γ^2, T) and (γ_0^2, T_0), respectively, then to the first order in $\delta(r,\varphi)$ we have for TM-modes

$$\gamma^2 - \gamma_0^2 = +\frac{\oint_{C_0}\delta(\varphi)|\frac{\partial T_0}{\partial n}|^2 dl_0}{\int_{S_0}|T_0(r,\varphi)|^2 dS_0} \quad , \tag{7}$$

where $\partial T/\partial n = \mathbf{n}\cdot\nabla T$ is the so-called normal derivative of T. In our case, the unperturbed transverse mode functions for TM-modes are given by (3). Performing the integrations in (7), we obtain

$$\gamma^2 - \gamma_0^2 = \frac{n^2\pi^2}{(R_O-R_I)^2}\,\frac{\varepsilon}{R_O-R_I}\,\delta_{n,1} \quad , \tag{8}$$

where $\delta_{n,1}$ is a Cronecker delta function and should not be confused with our deformation parameter $\delta(r,\varphi)$ or $\delta(\varphi)$. Thus we see that, to the first order of perturbation, only the TM-modes with $m = 1$, i.e. TM_{m1}-modes, give a non-zero deviation of the eigenvalues γ^2 from the unperturbed eigenvalue parameters γ_0^2. Using now the result (4) with $m = 1$, we obtain the perturbed eigenvalue parameters γ^2 in the form

$$\gamma^2_{n,m} = \frac{n^2\pi^2}{(R_O-R_I)^2}\left(1 + \frac{\varepsilon}{R_O-R_I}\right) + \frac{4}{(R_O+R_I)^2} \quad . \tag{9}$$

Thus, in the regions 1 and 2, as depicted in Fig. 2, the elliptic perturbation causes an effective decrease of R_1 and R_2, i.e.

$$R_1' = R_1 - \frac{\varepsilon}{2} \quad , \quad R_2' = R_2 - \frac{\varepsilon}{2} \quad . \tag{10}$$

On the other hand, the radii of the magnetic core and the tank wall are clearly not affected by the elliptic deformation of the winding segments (or turns). Thus in the regions 3 and 4, as depicted in Fig. 2, there are no effects of the elliptic perturbation and we can use the unperturbed eigenfunctions and eigenvalue parameters. We can therefore introduce a new variable $\rho = r - R_C$ and replace the mode numbers $(n, 1)$ simply by (n). Following [5], we define the orthonormal basis functions for $\mathrm{TM_n}$-modes ($\mathrm{TM_{n,1}}$-modes) in the regions 1 (below the conductive obstacle) and 2 (above the conductive obstacle) as follows

$$\psi_n^{(1)}(\rho,\varphi) = \sqrt{\frac{2-\delta_{n,0}}{\pi(R_1'-R_C)}}\cos\left(\frac{n\pi\rho}{(R_1'-R_C)}\right)\cos\varphi \quad , \tag{11}$$

$$\psi_n^{(2)}(\rho,\varphi) =$$

$$= \sqrt{\frac{2-\delta_{n,0}}{\pi(R_W-R_2')}}\cos\left[\frac{n\pi}{\pi(R_W-R_2')}(a-\rho)\right]\cos\varphi \quad , \tag{12}$$

while in the regions 3 and 4, with no obstacle present, the basis functions are equal to each other and given by

$$\psi_n^{(3)}(\rho,\varphi) = \psi_n^{(4)}(\rho,\varphi) =$$

$$= \sqrt{\frac{2-\delta_{n,0}}{\pi(R_W-R_C)}}\cos\left(\frac{n\pi\rho}{(R_W-R_C)}\right)\cos\varphi \quad . \tag{13}$$

Here we can use the definition of the transverse wave number γ_n in the lossless case ($\sigma = 0$), i.e. $\gamma_n^2 = \omega^2\mu\epsilon - k_{zn}^2$, where we denote the longitudinal wave number for the n-th mode by k_{zn}. Thus, the longitudinal wave numbers $k_{zn}^{(i)}$ and the TM_n-mode impedances $Z_n^{(i)}$ for the four regions (i = 1,2,3,4) can be written in the form

$$k_{zn}^{(i)2} = \omega^2\mu\epsilon - \gamma_n^{(i)2} = k^2 - \gamma_n^{(i)2} \quad , \tag{14}$$

$$Z_n^{(i)} = \frac{k_{zn}^{(i)}}{k}\eta \quad , \quad \eta = \sqrt{\frac{\mu}{\epsilon}} \quad . \tag{15}$$

The radial electric fields $E_{rn}^{(i)}$ and azimuthal magnetic fields $H_{\varphi n}^{(i)}$ are now linear combinations of the basis functions $\psi_n^{(i)}(\rho)$ for the respective region. These transverse fields can be expanded, in terms of the basis functions, as follows [8]:

$$E_r^{(i)}(\rho,\varphi,z) = \sum_{n=0}^{\infty}\left[c_n^{(i)+}(z) + c_n^{(i)-}(z)\right]Z_n^{(i)}\psi_n^{(i)}(\rho,\varphi) \quad , \tag{16}$$

$$H_\varphi^{(i)}(\rho,\varphi,z) = \sum_{n=0}^{\infty}\left[c_n^{(i)+}(z) - c_n^{(i)-}(z)\right]\psi_n^{(i)}(\rho,\varphi) \quad . \tag{17}$$

where for each mode and each region $E_{rn}^{(i)} = Z_n^{(i)}H_{\varphi n}^{(i)}$, while $c_n^{(i)\pm}(z)$ are coefficients for modes propagating in $\pm z$-direction. Here we need to consider the boundary conditions at the planes $z = z_1$ and $z = z_2$. First, we have the continuity of the transverse electric field component E_r over the entire surface, where $\mathbf{E} = \mathbf{0}$ inside the conductive material yields that E_r vanishes at the metallic part of the boundary. The second condition is that H_φ must be continuous over the aperture parts of the surface. In equations (16) and (17), the sum is performed over all modes ($0 \le n \le \infty$), but in the numerical implementation, each summation needs to be reduced from ∞ to a maximum mode number N_i ($i = 1,2,3,4$). Thus, with a finite number of modes ($0 \le n_i \le N_i$), we define the vectors $\mathbf{c}_{(i)}^{\pm}(z)$ by ($i = 1,2,3,4$)

$$\mathbf{c}_{(i)}^{\pm}(z) = \left[c_1^{(i)\pm}(z) \quad c_2^{(i)\pm}(z) \quad ... \quad c_{N_i}^{(i)\pm}(z)\right]^T \quad . \tag{18}$$

Following [5], the scattering analysis gives the following results

$$\begin{bmatrix} \mathbf{c}^-(z_\mathrm{L}) \\ \mathbf{c}^+(z_\mathrm{R}) \end{bmatrix} = \begin{bmatrix} \mathbf{S}_{11} & \mathbf{S}_{12} \\ \mathbf{S}_{21} & \mathbf{S}_{22} \end{bmatrix}\begin{bmatrix} \mathbf{c}^+(z_\mathrm{L}) \\ \mathbf{c}^-(z_\mathrm{R}) \end{bmatrix} \quad . \tag{19}$$

Thus we obtain the complete scattering matrix equation for propagation over one "cell", i.e. from z_L to z_R. The cascading of one cell denoted by a, with scattering matrix $\mathbf{S}^a$ and situated in the interval $z_1 \le z \le z_2$, with a neighboring cell denoted by b, with scattering matrix $\mathbf{S}^b$ and situated in the interval $z_2 \le z \le z_3$, gives the following scattering equation:

$$\begin{bmatrix} \mathbf{c}^-(z_1) \\ \mathbf{c}^+(z_3) \end{bmatrix} = \begin{bmatrix} \mathbf{S}_{11}^c & \mathbf{S}_{12}^c \\ \mathbf{S}_{21}^c & \mathbf{S}_{22}^c \end{bmatrix}\begin{bmatrix} \mathbf{c}^+(z_1) \\ \mathbf{c}^-(z_3) \end{bmatrix} \quad , \tag{20}$$

where

$$\mathbf{S}_{11}^c = \mathbf{S}_{11}^a + \mathbf{S}_{12}^a(\mathbf{I} - \mathbf{S}_{11}^b\mathbf{S}_{22}^a)^{-1}\mathbf{S}_{11}^b\mathbf{S}_{21}^a \tag{21}$$

$$\mathbf{S}_{12}^c = \mathbf{S}_{12}^a(\mathbf{I} - \mathbf{S}_{11}^b\mathbf{S}_{22}^a)^{-1}\mathbf{S}_{12}^b \tag{22}$$

$$\mathbf{S}_{21}^c = \mathbf{S}_{21}^b(\mathbf{I} - \mathbf{S}_{22}^a\mathbf{S}_{11}^b)^{-1}\mathbf{S}_{21}^a \tag{23}$$

$$\mathbf{S}_{22}^c = \mathbf{S}_{22}^b + \mathbf{S}_{21}^b(\mathbf{I} - \mathbf{S}_{22}^a\mathbf{S}_{11}^b)^{-1}\mathbf{S}_{22}^a\mathbf{S}_{12}^b \tag{24}$$

Using the cascading formula (20) with (21-24), it is possible to cascade together any number of cells by iteration.

IV. R

The computer simulation geometry of our transformer winding model is shown in Fig. 4. At this stage of our research, we are mainly concerned with investigating the diagnostic principles, such that the dimensions chosen in Fig. 4 are not intended to mimic any realistic power transformer. It should be noted that the elliptic deformations correspond to the radial extensions of winding segments or turns, as shown in Fig. 4. Such deviations are indeed frequently found when inspecting old decommissioned power transformers. Some typical mechanical deformations of winding segments are shown and studied using frequency response analysis (FRA) in e.g. [11]. The inverse problem to determine the studied parameters $\mathbf{x} = (\rho_1, \rho_2, ...\rho_n)$ is based on minimizing the optimization function J, defined by

$$J(\mathbf{x}) = \sum_{i,j}\left|\mathbf{S}_{ij}^{\mathrm{calc}}(\mathbf{x}) - \mathbf{S}_{ij}^{\mathrm{meas}}\right|^2 \quad , \tag{25}$$

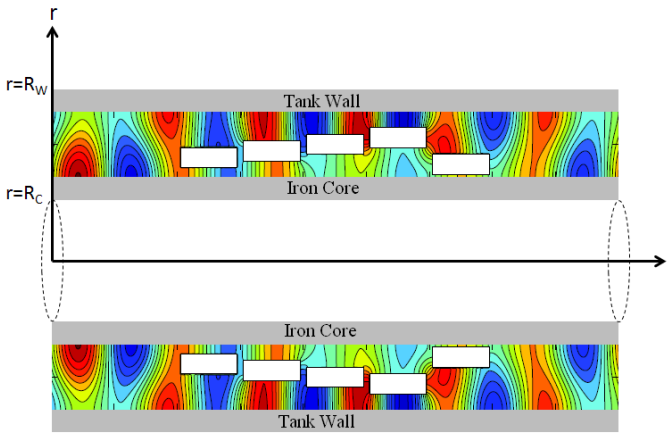

Fig. 4. The computer simulation geometry with a distance between the tank wall and magnetic core $R_W - R_C = 1$ m and five winding segments, each with width $R'_2 - R'_1 = 0.3$ m and height $z_2 - z_1 = 0.9$ m. The colors indicate the value of the resulting magnetic field H_φ when the lowest TM-mode of frequency $f = 200$ MHz is incident from the left.

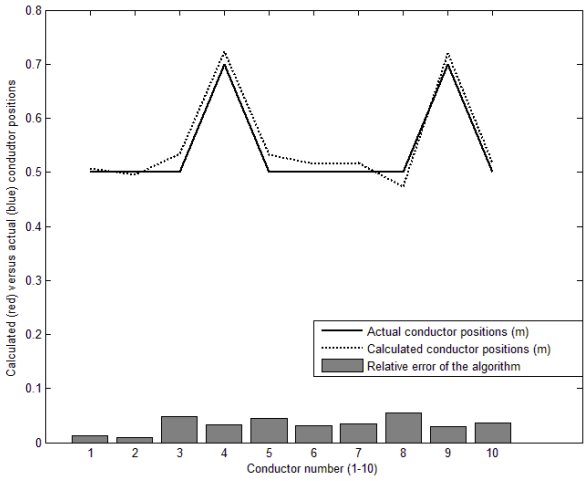

Fig. 5. Calculated (dotted line) versus actual (full line) conductor positions. for the case of ten conductor cells at $f = 250$ MHz

where $\mathbf{S}_{ij}^{\text{calc}}(\mathbf{x})$ are the elements of the calculated scattering matrix and $\mathbf{S}_{ij}^{\text{meas}}$ are the corresponding elements of the measured scattering matrix. In the present paper, the studied parameters are the radial positions of the winding segments that reflect the elliptic deformations according to the formulae (10). The optimization model is tested by comparing our calculated scattering data with synthetic measurement data generated from the commercial program HFSS. The S-parameters are determined directly from HFSS by using the three lowest wave modes and defining two ports at the two sides of the waveguide. Here we present a case of reconstruction of 10 conductors, where two of the conductors are subject to elliptic deviations. The results are shown in Fig. 5, where we obtained good reconstruction results for the effective winding positions that reflect the corresponding elliptic deformations according to the formulae (10).

V. C

We studied elliptic deformations of winding turns in a power transformer using the first-order perturbation theory. We simulated antennas inside the transformer tank to radiate and measure microwave fields in order to identify and quantify elliptic deformations of the individual winding segments or individual turns. Using optimization to solve the inverse problem, we obtained a good agreement between the reconstructed and true deformations of the winding segments.

A

This work was funded by the Swedish Energy Agency, Project Nr 34146-1.

R

[1] E.A. Mackenzie, J. Crossey, A. de Pablo, W. Ferguson, "On-line monitoring and diagnostics for power transformers", Electrical Insulation (ISEI), *Conference Record of the 2010 IEEE International Symposium* , pp. 1-5, San Diego, CA, 6-9 June 2010.

[2] P.T.M. Vaessen, E. Hanique: "A New Frequency Response Analysis Method for Power Transformers", *IEEE Transactions on Power Delivery*, Vol .7, N 1, pp. 384 391, January 1992.

[3] Y. Shao, Z. Rao, Z. Jin, "Online State Diagnosis of Transformer Windings Based on Time-frequency Analysis", *WSEAS Transactions on Circuits and Systems*, Issue 2, Volume 8, pp. 227-236, February 2009.

[4] Abeywickrama N., Serdyuk Y. V., Gubanski S. M., "High-Frequency Modeling of Power Transformers for Use in Frequency Response Analysis (FRA)", *IEEE Trans. On Power Delivery*, Vol. 23, No. 4, pp. 2042 2049, 2008.

[5] M. Dalarsson, A. Motevasselian, M. Norgren, "On Using Multiple Modes to Reconstruct Conductor Locations in a Power Transformer Winding", *PIERS 2012 Proceedings* , Kuala Lumpur, Malaysia, March 27-30, pp. 516-523, 2012.

[6] R. Myska and P. Drexler, "Simulation and Verification of Methods for Partial Discharge Source Localization", *PIERS 2012 Proceedings* , Kuala Lumpur, Malaysia, March 27-30, pp. 704-708, 2012.

[7] Colton D. and Kress R., Inverse Acoustic and Electromagnetic Scattering Theory, *Springer*, Berlin, 1992

[8] P. H. Masterman and P. J. B. Clarricoats, "Computer Field-Matching Solution of Waveguide Transverse Discontinuities", *Proc. IEEE*, Vol. 118, 51 63, 1971.

[9] J.D. Jackson, "Classical Electrodynamics", Third Edition, *Wiley*, New York (1999)

[10] S.A. Schelkunoff, "Electromagnetic Waves", *D. Van Nostrand Company, Inc.*, New York (1943)

[11] L. Yanming, L. Gang, Z. Linhai, Z. Longjun and L. Zhiming, "Transformer Winding Deformation Diagnosis Using Middle Band Frequency Response Analysis", 2007 International Conference on Solid Dielectrics, Winchester, UK, July 8-13, pp. 677-680, 2007.